APPENDIX H

Multiplicities of Secondaries in Nuclear Interactions, Induced by ^{20}Ne, ^{40}Ar and ^{56}Fe Nuclei at 0.1-0.5 GeV/Nucleon

by

V.E. Dudkin, E.E. Kovalev, N.A. Nefedov, V.A. Antonchik
S.D. Bogdanov, V.F. Kosmach, A.Yu. Likhachev, J. Hassan
E.V. Benton and H.J. Crawford

Nuclear Physics A568 (1994) 906–916
North-Holland

NUCLEAR
PHYSICS A

Multiplicities of secondaries in nuclear interactions, induced by ^{20}Ne, ^{40}Ar and ^{56}Fe nuclei at 0.1–0.5 GeV/nucleon

V.E. Dudkin, E.E. Kovalev, N.A. Nefedov

Research Test Center for Radiation Safety of Space Flights of the Ministry of Public Health of Russia, 123182 Moscow, Russian Federation

V.A. Antonchik, S.D. Bogdanov, V.F. Kosmach, A.Yu. Likhachev, J. Hassan

St. Petersburg State Technical University, St. Petersburg, Russian Federation

E.V. Benton [1]

Physics Department, University of San Francisco, San Francisco, CA 94117-1080, USA

H.J. Crawford

University of California Space Sciences Laboratory, Berkeley CA 94720, USA

Received 26 October 1992
(Revised 23 June 1993)

Abstract

Multiplicities of various species of charged secondaries produced in inelastic interactions of ^{20}Ne, ^{40}Ar and ^{56}Fe nuclei with emulsion nuclei at 0.1–0.5 GeV/nucleon have been measured. The data obtained are compared with the results for interactions of higher energy nuclei with emulsion nuclei. The dependences of the nucleus–nucleus interaction parameters on masses and energies of colliding nuclei are examined.

Key words: NUCLEAR REACTIONS Em(^{20}Ne, X), $E = 0.28$ GeV/nucleon; Em(^{40}Ar, X), $E = 0.27$ GeV/nucleon; Em(^{56}Fe, X), $E = 0.48$ GeV/nucleon; measured σ_{in}, mean multiplicities $\langle n_i \rangle$ of charged secondaries in reactions with hydrogen, light (C, N, O) and heavy (Ag, Br) target nuclei. Examined the relationship $\langle n_i \rangle$ (E, A_p, A_t).

[1] USF portion of the work partially supported by NASA Grant No. NAG9-235, NASA-Johnson Space Center, Houston.

SSDI 0375-9474(93)E0433-9

1. Introduction

Photoemulsion measurements of secondary-particle multiplicities in nuclei-induced interactions below 1 GeV/nucleon have had a revival of interest among researchers recently [1]. Copious data have been obtained on interactions of nuclei of relativistic and ultra-relativistic velocities [2–5], so the necessity has arisen for deriving comparative data measured by identical techniques, but at lower projectile velocities.

The present work provides new experimental data on interactions of Ne, Ar and Fe nuclei at lower energies with emulsion nuclei and analyzes the effect of projectile velocity on the basic characteristics of a nucleus–nucleus interaction event.

2. Experimental design

Photoemulsion (Em) chambers assembled of Russian-manufactured nuclear emulsion BR-2 layers were irradiated by 0.39 GeV/nucleon ^{20}Ne, 0.48 GeV/nucleon ^{40}Ar, and 0.583 GeV/nucleon ^{56}Fe nuclei at the BEVALAC accelerator of the University of California, Berkeley. The layers were developed and marked at the High Energy Laboratory of JINR (Dubna). The interactions were sought by double inspection of tracks at a 60×15 magnification. The average ranges of stopping ions were 61.75 ± 0.06 mm for 0.39 GeV/nucleon ^{20}Ne ions, 53.11 ± 0.05 mm for 0.48 GeV/nucleon ^{40}Ar ions, and 45.45 ± 0.04 mm for 0.583 GeV/nucleon ^{56}Fe ions. These ranges can be approximated by the range–energy dependence for multiply charged ions [6,7], thereby permitting the energies of projectile nuclei to be determined at the points of their interactions with photoemulsion nuclei. The error in finding the energy of a split-inducing nucleus did not exceed 1%. Accuracy in the finding of the projectile energy in the interaction point is due to the very small spread of the BEVALAC beam energy. Determined from the stopping ion range distributions, experimental stragglings were $(0.95 \pm 0.06)\%$, $(0.96 \pm 0.05)\%$ and $(0.42 \pm 0.02)\%$ for ^{20}Ne, ^{40}Ar and ^{56}Fe ions, respectively. These stragglings proved to be more than theoretical values: 0.26%, 0.16% and 0.14% calculated according to Barkas et al. [8] for the ions mentioned above. At the same time, the results obtained showed the possibility of accurately defining the projectile energy in the interaction point by measuring the particle path in emulsion before collision and using the range–energy dependence for heavy ions. The ranges of nuclei of different energies and charges calculated by these techniques [6–9] were also used to identify secondaries.

The total statistics of the recorded events were 436 (^{20}Ne + Em, $E_0 = 0.1$–0.39 GeV/nucleon (the mean value of projectile energy $\langle E_0 \rangle = 220 \pm 20$ MeV/nucleon)), 396 (^{40}Ar + Em, $E_0 = 0.1$–0.48 GeV/nucleon ($\langle E_0 \rangle = 270 \pm 20$ MeV/

Table 1
Experimental statistics of events used for present analysis

Projectile	$\langle E_0 \rangle$ (MeV/nucleon)	Target	Number of events
^{20}Ne	220 ± 20	H	37
		CNO	96
		AgBr	163
^{40}Ar	270 ± 20	H	23
		CNO	63
		AgBr	116
^{56}Fe	480 ± 20	H	71
		CNO	218
		AgBr	322

nucleon)), and 1005 (^{56}Fe + Em, $E_0 = 0.1$–0.58 GeV/nucleon ($\langle E_0 \rangle = 480 \pm 20$ MeV/nucleon)), while the mean free paths for interaction were 11.99 ± 0.58 cm, 10.07 ± 0.57 cm and 8.19 ± 0.26 cm, respectively. A number of events (1, 109) were selected randomly from the overall statistics of the detected collisions and were then processed by the standard techniques [2,3]. The species of target-nuclei were found and the energies and changes of all secondaries were determined. The statistics used for our analysis are presented in Table 1.

3. Interaction cross sections

The experimental interaction paths of Ne, Ar and Fe nuclei, the numbers of interactions with a selected species of target nuclei, and concentrations of individual nuclei in emulsion [10] were used to find the cross sections for inelastic

Table 2
Total inelastic cross sections (mb)

Projectile		Target					
ion	energy (GeV/nucleon)	H	C	N	O	Br	Ag
Ne	0.22	330 ± 60	930 ± 100	990 ± 110	1040 ± 110	2060 ± 170	2380 ± 190
	3.6 [a]	360 ± 70	960 ± 110	1030 ± 120	1090 ± 130	2260 ± 210	2650 ± 240
Ar	0.27	360 ± 80	1070 ± 140	1130 ± 150	1190 ± 150	2590 ± 240	2930 ± 280
	1.1 [b]	510 ± 90	1190 ± 150	1260 ± 150	1330 ± 150	3020 ± 270	3480 ± 290
Fe	0.48	450 ± 60	1540 ± 110	1580 ± 120	1630 ± 130	2820 ± 300	3230 ± 340
	1.8 [c]	740 ± 70	1750 ± 110	1800 ± 120	1860 ± 130	3090 ± 260	3300 ± 280

[a] See ref. [11].
[b] See ref. [3].
[c] See ref. [2].

interactions with particular emulsion nuclei (see Table 2). Table 2 also presents the experimental data [2,3,11] obtained at higher energies. From the comparison it is seen that, as the projectile energy increases from a few hundred MeV/nucleon to a few GeV/nucleon, the cross sections also increase; that is in agreement with the data of the experiment by Webber et al. [12] and Chen et al. [13]. In the early experiments with < 1 GeV/nucleon nuclei, the nuclear interaction cross sections for $p + A$ collisions were noted to increase with increasing projectile mass more rapidly than in A–A reactions. In our experiment the difference in the increases is less perceptible. The approximation of the cross sections for non-relativistic and relativistic interactions by the Bradt–Peters formula:

$$\sigma = \pi R_0^2 \left[A_p^{1/3} + A_t^{1/3} - \beta_0 \left(A_p^{-1/3} + A_t^{-1/3} \right) \right]^2, \tag{1}$$

using the least squares method, has yielded $R_0 = 1.27 \pm 0.03$ fm, $\beta_0 = 1.14 \pm 0.11$; $\chi^2/k = 0.8$, and $R_0 = 1.28 \pm 0.01$ fm, $\beta_0 = 0.75 \pm 0.05$; $\chi^2/k = 1.81$, for energies of 0.1–0.5 GeV/nucleon and above 1.0 GeV/nucleon, respectively. In the case of relativistic interactions, the factors R_0 and β_0 proved to be close to those presented in ref. [14] which summarized the data on the interactions of nuclei with energies above 1 GeV/nucleon ($R_0 = 1.32 \pm 0.01$ fm and $\beta_0 = 0.85 \pm 0.03$). It should be noted that at both $E_0 \geqslant 1$ GeV/nucleon and $E_0 = 0.1$–0.5 GeV/nucleon, the R_0 value, which characterizes the radii of interacting nuclei, remains constant. The only variable is the overlap parameter β_0 which rises with decreasing projectile energy. This means that the interacting nuclei become more transparent at $E_0 = 0.1$–0.5 GeV/nucleon. Such a variation in β_0 (at a constant R_0 value) is not a trivial result and seems to us to necessitate further experimental studies [15].

4. Multiplicities of secondaries

The experiments discriminate between slow target fragments (b-particles, with $E_p \leqslant 26$ MeV), fast fragments of a target nucleus (g-particles, with $26 < E_p < 400$ MeV), "shower" particles (s-particles, with $E_p > 400$ MeV and $E_\pi > 60$ MeV, which are interacting projectile protons and produced π-mesons), s′-particles (which are relativistic singly charged fragments of a projectile nucleus with $E_p < 26$ MeV in the system of the projectile and which are excluded from the number of s-particles), g′-particles (which are projectile fragments with $Z = 2$), and b′-particles (which are projectile fragments with $Z \geqslant 3$). In addition, the total charge Q of the non-interacting projectile fragments was found.

Fig. 1 shows the laboratory relative-rapidity distribution Y/Y_0 ($Y = \frac{1}{2}\ln[(E + P_\parallel)/(E - P_\parallel)]$; Y_0 is the projectile rapidity) of the examined particles for interactions of argon nuclei with light and heavy nuclei at non-relativistic and relativistic velocities of a projectile. The statistics presented in Antonchik et al. [3], where the

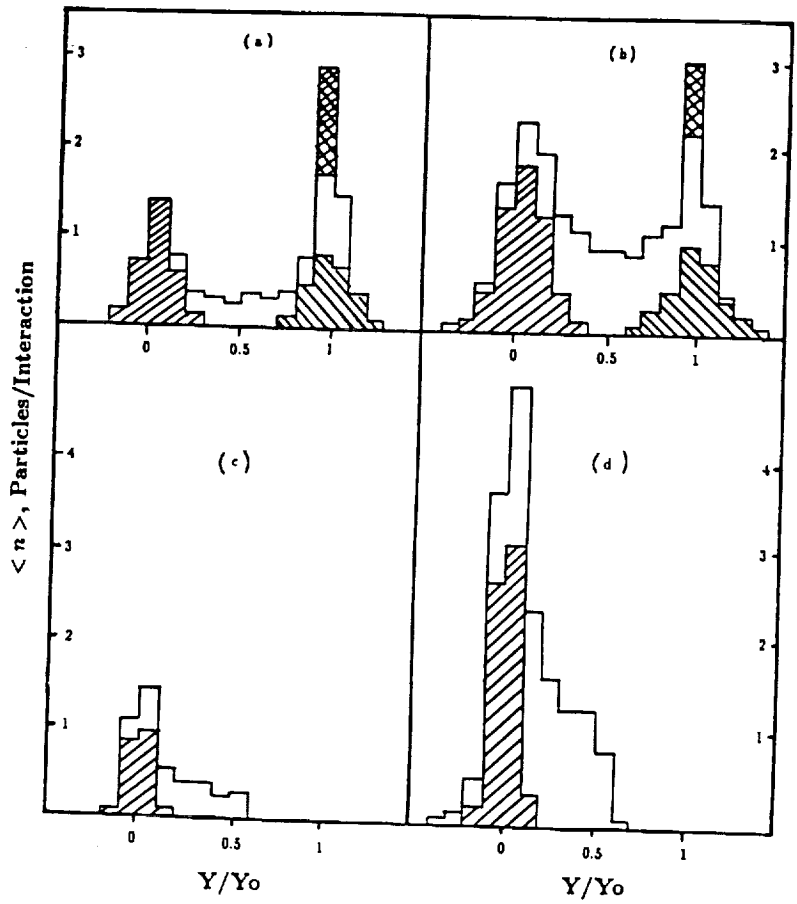

Fig. 1. Relative-rapidity (Y/Y_0) distributions (Y_0 is the projectile rapidity) for (a) the interactions ^{40}Ar + C, N, O and (b) ^{40}Ar + Ag, Br at energy 0.27 GeV/nucleon, and for (c) interactions ^{40}Ar + C, N, O and (d) ^{40}Ar + Ag, Br at a 1.1 GeV/nucleon projectile energy. The non-shaded area indicates g- and s-particles; right-inclined hatches represent b-particles; left-inclined hatches are for (s′ + g′)-particles; and the doubly shaded area is for multiply charged ($Z \geq 3$) fragments. For projectile energy 1.1 GeV/nucleon (c, d), only distributions corresponding to b- and g-particles are shown.

energies of secondaries were found for the b- and g-particles only, were for the case of relativistic nuclear interactions. The distributions presented in Figs. 1a, b exhibit two pronounced peaks due mainly to the b- and (s′ + g′)-particles, i.e. the particles emitted from an excited residual target nucleus (b-particles, $Y/Y_0 \simeq 0$) and from a projectile residue (s′- and g′-particles, $Y/Y_0 \simeq 1$). An additional contribution to the peak at $Y/Y_0 \simeq 1$ is from the projectile fragments (b′-particles) which may be treated as residues of a given nucleus on completing the slow stage. The non-shaded area (g-particles at $Y/Y_0 < 0.5$ and s-particles at $Y/Y_0 > 0.5$) is mainly located within the 0.1–0.9 relative-rapidity range and fills the gap between two peaks. From Fig. 1 it follows that, as regards the kinematic parameters, the b- and g-particles may be attributed to the target nucleus, and the b′-, g′-, s′- and s-particles to the projectile nucleus, although the correlation of the g- and

Table 3
Mean multiplicities of secondaries in non-relativistic interactions

Reaction type	$\langle n_b \rangle$	$\langle n_g \rangle$	$\langle n_s \rangle$	$\langle n_{s'} \rangle$	$\langle n_{g'} \rangle$	$\langle Q \rangle$	$\langle n_{in} \rangle$
Ne + H	0.14 ± 0.06	0.59 ± 0.08	0.54 ± 0.12	1.43 ± 0.20	1.03 ± 0.17	9.73 ± 0.12	0.5 ± 0.2
Ne + CHO	2.89 ± 0.12	1.54 ± 0.15	1.67 ± 0.16	1.69 ± 0.13	1.45 ± 0.13	8.35 ± 0.17	3.3 ± 0.4
Ne + AgBr	5.31 ± 0.42	3.54 ± 0.32	2.08 ± 0.17	1.53 ± 0.10	1.02 ± 0.08	7.50 ± 0.22	5.0 ± 0.5
Ne + Em	3.88 ± 0.25	2.52 ± 0.19	1.75 ± 0.11	1.57 ± 0.08	1.16 ± 0.07	8.06 ± 0.14	3.9 ± 0.3
Ar + H	0.61 ± 0.10	0.17 ± 0.08	0.26 ± 0.09	1.00 ± 0.21	0.35 ± 0.13	17.74 ± 0.11	0.6 ± 0.2
Ar + CNO	2.94 ± 0.17	1.16 ± 0.15	1.67 ± 0.23	2.33 ± 0.19	1.38 ± 0.15	16.65 ± 0.21	3.0 ± 0.4
Ar + AgBr	5.87 ± 0.48	4.38 ± 0.51	3.57 ± 0.34	2.78 ± 0.16	1.47 ± 0.12	14.25 ± 0.41	8.3 ± 0.9
Ar + Em	4.36 ± 0.31	2.90 ± 0.32	2.60 ± 0.22	2.44 ± 0.11	1.32 ± 0.09	15.40 ± 0.26	5.8 ± 0.5
Fe + H	0.36 ± 0.07	0.62 ± 0.16	1.06 ± 0.23	1.94 ± 0.28	1.02 ± 0.18	25.62 ± 0.35	0.8 ± 0.7
Fe + CNO	2.43 ± 0.14	2.26 ± 0.17	3.04 ± 0.24	3.46 ± 0.21	1.92 ± 0.12	22.18 ± 0.29	8.2 ± 0.6
Fe + AgBr	7.98 ± 0.38	8.17 ± 0.69	5.79 ± 0.47	3.38 ± 0.21	1.77 ± 0.12	19.55 ± 0.59	13.9 ± 1.2
Fe + Em	5.11 ± 0.27	5.18 ± 0.31	4.26 ± 0.34	3.24 ± 0.20	1.74 ± 0.11	21.19 ± 0.32	10.4 ± 0.7

s-particles with the respective nuclei is less stringent when compared with the case of b- and (s′ + g′)-particles.

Table 3 presents the mean multiplicities of the above-mentioned particles and shows the estimates of the number of the projectile nucleons involved in an interaction:

$$\langle n_{\text{in}} \rangle = A_{\text{p}} - \frac{A_{\text{p}}}{Z_{\text{p}}} \langle Q \rangle, \tag{2}$$

where A_{p} and Z_{p} are the projectile mass and charge numbers, respectively.

From Table 3 it follows that the non-relativistic nucleus–nucleus collisions exhibit some of the features found when studying the > 1 GeV/nucleon nuclear interactions [2,4,16,17], namely:

(1) the mean number of the interacting projectile nucleons $\langle n_{\text{in}} \rangle$ increases with target-nucleus mass;

(2) the singly-to-doubly charged projectile fragment ratio $\langle n_{s'}/n_{g'} \rangle$ is defined mainly by the projectile species and depends very little on the target mass;

(3) the specific multiplicities of the charged secondaries of all species, $\langle n_i \rangle / \langle n_{\text{in}} \rangle$, where subscript i is the type of secondary, prove to be below the respective mean multiplicities for the interactions of protons of the same velocities with emulsion nuclei;

(4) as the masses of interacting nuclei increase, the multiplicities of all particle species are observed to rise.

Thus, the analysis of the data has shown that the projectile energy decrease from 3.6 to 0.3 GeV/nucleon does not result in any variation of the qualitative behavioral features of the multiplicities of secondaries.

We used the data of Table 3, as well as the experimental results for 3.6 GeV/nucleon protons, carbon and oxygen [16], 3.2 GeV/nucleon ^{22}Ne [4], 1.1 GeV/nucleon ^{40}Ar [3], and 1.8 GeV/nucleon ^{56}Fe [2] beams, to study the mean multiplicities of the identified species of secondaries as a function of the masses and energies of colliding nuclei on the assumption that, on average, ^{14}N and ^{94}Nb are the light and heavy emulsion nuclei, respectively [17]. The dependence on the nuclear masses and energies was taken to be

$$\langle n_i \rangle = \alpha_0 A_{\text{p}}^{\alpha_{\text{p}}} A_{\text{t}}^{\alpha_{\text{t}}} E_0^{\alpha_{\text{E}}}, \tag{3}$$

where A_{p} and A_{t} are the mass numbers of projectile and target, respectively; E_0 is the projectile kinetic energy in GeV/nucleon. Parametrization of the above type is used frequently to study nucleus–nucleus interactions. The factor α_0 and power exponents α_{p}, α_{t} and α_{E} were determined by the nonlinear least squares method for the case of different precision measurements [18]. The zero approximation was selected from the linear approximation (by taking the logarithm in the right part of

Table 4
Coefficients of approximation of the dependence (3), obtained by least squares method

Particle type	α_0	α_p	α_t	α_E	χ^2_{23}
$\langle n_b \rangle$	0.28 ± 0.04	0.03 ± 0.03	0.68 ± 0.02	−0.12 ± 0.02	216
$\langle n_{s'} + n_{g'} \rangle$	0.32 ± 0.04	0.58 ± 0.04	0.07 ± 0.03	−0.07 ± 0.02	261
$\langle n_g \rangle$	0.037 ± 0.008	0.51 ± 0.05	0.81 ± 0.03	0.34 ± 0.03	114
$\langle n_s \rangle$	0.21 ± 0.04	0.52 ± 0.05	0.39 ± 0.02	0.70 ± 0.03	79
$\langle Q \rangle$	0.49 ± 0.02	0.97 ± 0.02	−0.06 ± 0.01	−0.033 ± 0.004	149
$\langle n \rangle$	1.38 ± 0.13	0.34 ± 0.03	0.38 ± 0.03	0.27 ± 0.02	185

Eq. (3)). The approximation was calculated (stoppage of the program) if the decrease in value of the residual sum of the squares in the kth step was smaller than 1%.

The errors (covariational matrix) of the sought factor and exponents were determined by means of linear approximation using the matrix of derivatives at the point of the $(k-1)$th approximation. The relative error of the initial data (of the multiplicities of different-species particles) was some 5–10%. In the case of the 27 experimental points which we have described by parametrization (3) (four unknowns), the relative error in the unknowns proved to be reduced, on average, by a factor of two to three, depending on the particular values of the matrix of derivatives at the point of the $(k-1)$th approximation.

The values obtained for the unknowns in parametrization (3), to be used to describe the dependence of the mean multiplicities of different-species particles, are presented in Table 4 which also shows values of the normalized sum of squares χ^2_{23} together with the values of the approximation coefficients for the mean multiplicity of all charged particles in an interaction $\langle n \rangle$.

We examine some of the dependences obtained. The b-particle multiplicity is characterized by an extremely weak dependence on A_p. As a nucleus–nucleus collision energy increases, the decrease of the mean multiplicity of b-particles becomes perceptible (the α_E value is negative). In the case of "evaporation" particles from a projectile residue $\langle n_{s'} + n_{g'} \rangle$ we again observe that any dependence on the mass of a collision partner nucleus in practice is absent and that the α_E value is negative. It seems to us that the similarity (to within experimental errors) among all the approximation coefficients for $\langle n_b \rangle$ and $\langle n_{s'} + n_{g'} \rangle$ (allowing the substitution of A_p for A_t) is indicative of identical mechanisms of the generation of these particular particle species (see also Fig. 1). The multiplicity of the g-particles, which are mostly target protons having interacted with some of the projectile nucleons, depends strongly on the target mass. The $\langle n_g \rangle / \langle n_b \rangle$ ratio characterizing the energy spectrum of target-emitted secondaries rises with an increase in both the projectile size, $\sim A_p^{0.48}$, and the target size $\sim A_t^{0.13}$. The energy dependence of the g-particle multiplicity in nucleus–nucleus interactions ($\alpha_E = 0.34 \pm 0.03$) has proved to be much weaker than in proton–nucleus interactions

($\alpha_E = 0.70$ [17]), contrary to the consequences of the simple superposition models which assume that the nucleus–nucleus interactions can be treated as a non-coherent sum of nucleon–nucleus, or even nucleon–nucleon, collisions. On the contrary, the multiplicity of s-particles (the generated pions included) exhibits an E_0-dependence close to that observed in the proton–nucleus interactions ($\alpha_E = 0.70 \pm 0.03$ and $\alpha_E = 0.70$, respectively). From Table 4 it follows that the mean total charge of non-interacting projectile fragments (this value characterizes a projectile residue after the rapid stage) decreases with increase in the partner-nucleus mass [2] and/or with increasing interaction energy: $\alpha_t < 0$, $\alpha_E < 0$. We are of the opinion that the dependence $\langle Q \rangle (E_0)$ observed at the 0.3–3.6 GeV/nucleon range may reflect the energy dependence of the nucleon–nucleon interaction cross section in this particular energy range. At ~ 0.3 GeV/nucleon the nucleon–nucleon interaction cross sections run through their minimum, so the interacting nuclei prove to be most transparent.

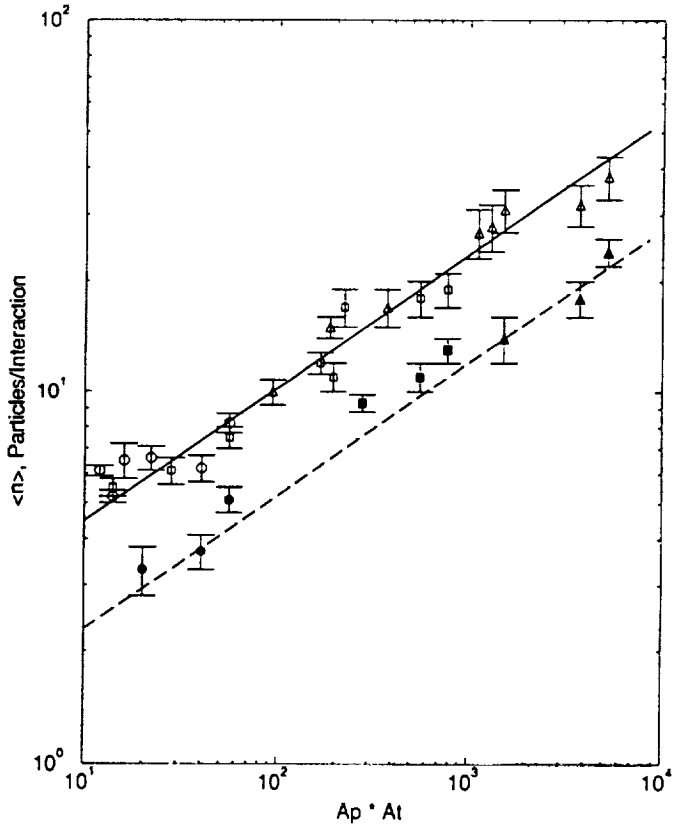

Fig. 2. The mean total multiplicity of all charged particles in an interaction versus the product of mass numbers of colliding nuclei and projectile energy. The symbols: ●, ○ = interactions with hydrogen; ■, □ = interactions with C, N, O, and ▲, △ = interactions with Ag, Br. The filled-in symbols (●, ■, ▲) and open symbols (○, □, △) correspond to projectile energies 0.1–0.5 GeV/nucleon and 1.8–3.6 GeV/nucleon, respectively. The solid and dashed lines are Eq. (3) approximations for energies 3.6 and 0.3 GeV/nucleon, respectively, and $\alpha_p = \alpha_t = 0.36$.

It is of great interest to examine the feasibility of describing the dependences of the total multiplicity of all charged particles in an interaction $\langle n \rangle = \langle n_b + n_g + n_s + n_{s'} + n_{g'} + n_{b'} \rangle$ on energies and masses of colliding nuclei. From Table 4 it is seen that the power-law exponents α_p and α_t of the dependences equal 0.38 ± 0.03 and 0.34 ± 0.03, respectively, i.e. exponents are the same to within the experimental errors. In its turn, the result obtained permits the mean multiplicity of all charged particles in interactions $A_p + A_t$ and $A_t + A_p$ to be regarded as identical, i.e. the effect of the mass of a colliding nucleus is of the same character, irrespective of whether the nucleus is a projectile or a target.

Since the total multiplicity $\langle n \rangle$ includes not only the recoil nucleus and evaporation particles (the particles already in nuclei), but also the newly generated mesons, the result obtained cannot be regarded as trivial, although the high χ^2_{23} value is indicative of poor applicability of the simple power-law model to describing the interaction of two nuclei.

Fig. 2 illustrates the feasibility of examining the dependence of the total multiplicity of secondaries on only two, rather than three (A_p, A_t and E) parameters, namely, on the product of the masses of colliding nuclei ($A_p \times A_t$) and on the projectile energy. The values of the total multiplicities (except those obtained in this work) have been borrowed from refs. [2–4,10,14,15,19,20]. The lines in Fig. 2 represent $\alpha_p = \alpha_t = 0.36$ at $E_0 = 0.30$ and 3.6 GeV/nucleon. The dependence (Eq. (3)) describes the data quite well.

5. Conclusions

Analyzing the available experimental and calculated data has shown that:

(1) a decrease of a projectile energy from a few GeV/nucleon to hundreds of MeV/nucleon gives rise to a 10–15% decrease in the total nuclear interaction cross section and, hence, to an increased mean-free path of projectile nuclei;

(2) in the non-relativistic energy range, the interactions involve a smaller degree of destruction of colliding nuclei;

(3) the multiplicity of the particles (b, s′, g′) emitted during the slow interaction stage is defined unambiguously by the mass of the parent nucleus, and also depends little on the mass and energy of partner nuclei;

(4) the 3.6–0.3 GeV/nucleon variation of a projectile energy fails to alter the form of secondary-particle multiplicity dependence on the masses of interacting nuclei.

The authors are indebted to the personnel of the Berkeley BEVALAC and of the JINR High Energy Laboratory for enabling the photoemulsions to be studied; we are also grateful to laboratory workers who shared with us the burden of searching for events.

References

[1] B. Jakobsson et al., Nucl. Phys. A509 (1990) 195
[2] V.E. Dudkin, E.E. Kovalev, N.A. Nefedov, V.A. Antonchik, S.D. Bogdanov, V.I. Ostroumov, H.J. Crawford and E.V. Benton, Nucl. Phys. A509 (1990) 783
[3] V.A. Antonchik et al., Yad. Fiz. (Sov. J. Nucl. Phys.) 51 (1990) 765
[4] A-ABGDDEKLMRTU-B Collaboration, Yad. Fiz. (Sov. J. Nucl. Phys.) 45 (1987) 123
[5] G. Singh et al., Phys. Rev. Lett. 61 (1988) 1073
[6] W. Galbraith et al., High energy and nuclear physics data handbook (Chilton, Didcot, UK, 1963)
[7] H.H. Heckman et al., Phys. Rev. C117 (1960) 544
[8] W.H. Barkas et al., Phys. Rev. 98 (1955) 605
[9] V.E. Dudkin, E.E. Kovalev, N.A. Nefedov, V.A. Antonchik, S.D. Bogdanov, V.I. Ostroumov, E.V. Benton and H.J. Crawford, Nucl. Phys. A530 (1991) 759
[10] VLGKLMT Collaboration, Joint Institute of Nuclear Research report JINR R1-8313 (Dubna, 1974)
[11] A.V. Belousov, Summary of thesis for Candidate's Degree (Leningrad, 1984)
[12] W.R. Webber et al., Phys. Rev. C41 (1990) 520
[13] C.-X. Chen et al., Proc. XXII Int. cosmic ray conf. (ICRC), Vol. 2, Dublin, 1991 (Leeds Univ. Press, Leeds, UK, 1992) p. 296
[14] All-union state standard, GOST 25645.212-85 (Standardizdat, Moscow, 1986)
[15] Hoang, Cork and H.J. Crawford, Z. Phys. C29 (1985) 611
[16] V.A. Antonchik et al., Yad. Fiz. (Sov. J. Nucl. Phys.) 39 (1984) 1228
[17] V.S. Barashenkov and V.D. Toneev, Interactions of high energy particles and atomic nuclei with nuclei (Atomizdat, Moscow, 1972)
[18] V.N. Grishin et al., Mathematical processing and interpretation of physics experiments (Moscow State University Editorial Board, Moscow, 1988)
[19] DELTW Collaboration, Nucl. Phys. A208 (1973) 626
[20] K.G. Gulamov et al., Dokl. Akad. Nauk UzSSR 2 (1977) 20